Timber/Glass Adhesively Bonded I-beams

Louise Blyberg and Erik Serrano

November 2010

Linnæus University
School of Engineering

Investing in your future

EUROPEAN
UNION
European Regional
Development Fund

Preface

This report is the result of research performed within a project dealing with the combination of timber and glass in structural building components. The official name of the project is ”Glas och trä i samverkan — Innovativa byggprodukter med mervärde” (In English: “Glass and Timber — Innovative Building Components with Added-Value”).

The research project is coordinated by Glafo Glass Research Institute, and is subdivided into three main work packages dealing with mechanical behaviour of glass/timber composites (partly reported here), with energy and life cycle issues of the glass/timber components and with architectural aspects on the use of glass/timber composites in load bearing structures.

Financing of project is provided partly by the European Union's structural fund for regional development through the Swedish Agency for Economic and Regional Growth (Tillväxtverket). In addition, financing is provided by Linnæus University, Glafo AB and Lund University. The support from all these organisations is gratefully acknowledged.

Abstract

Timber and glass are materials with aesthetically pleasing properties. If the materials can be combined appropriately, drawbacks can be overcome and the beneficial mechanical properties utilised and timber/glass elements can be a natural part of the load-carrying structure of buildings. Since glass is a brittle material, an important task for the timber is the redundancy – a glass failure should not lead to a catastrophic failure of the entire structural element.

This paper presents results from ongoing research related to load-bearing components made of timber and glass. Results from tests on small timber/glass bond-line specimens, recently published in a technical report, are briefly presented[1]. The core of the paper is, however, a study of four-point bending tests on fourteen timber/glass I-beams. These I-beams had a nominal height of 240mm and were designed with a web of 10mm float glass and flanges of LVL (laminated veneer lumber), bonded together mainly with an acrylate adhesive.

The mean values of the twelve beams with acrylate adhesive imply that the ultimate load capacity is 240% of the load when the first crack in the glass appeared. Thus, the timber well fulfills the redundancy task of avoiding a catastrophic failure of the structural element.

---

[1] Currently not included, please refer to [1] instead

Contents

1 Introduction and previous work

This paper is a result of work performed within a project dealing with the combination of timber and glass in structural building components. The official name of the project is ‘Glas och trä i samverkan - innovativa byggprodukter med mervärde’. It has financing from the European Union’s structural fund for regional development, managed by Tillväxtverket.

There are quite a few examples where glass is used in structures even in load carrying elements. Studies where other materials are added as reinforcement and a way to build in a redundancy in the member can be found for steel [5], [6] and for wood [3]. The number of existing studies on timber-glass composites is limited, but an important characteristic property apparent in many of the studies is the redundancy which can be built into the element, glass failure does not necessarily lead to a catastrophic failure of the entire element. Another possible concept, noted by [3], is to use wood as load introducing material at supports and at joints between components.

The present work is a study of timber-glass beams with an I-shaped cross section, where the flanges are of LVL (laminated veneer lumber) and the web of glass. The main adhesive used for the beams here was studied on small-scale specimens within the same project [1].

Timber-glass I-beams of similar designs have been studied in previous work by Hamm [2] and also used in the construction of a hotel in Switzerland [4].

2 Methods

2.1 Materials and dimensions

A total of fourteen I-beam specimens with glass webs and wooden flanges were produced and tested. Three different adhesives and two different flange groove widths were used. The third modified parameter was whether or not the corners of the glass cross section were grinded (roughly polished) or not. Each beam is here presented with a three-letter label specifying which of these options that were employed. Table 1 presents this notation system.

2.1.1 Adhesives

SikaFast is a two-component adhesive based on ADP-technology (acrylic double performance) and cures by polymerisation. In the SikaFast series, there are three different adhesives 5211, 5215 and 5221 whose main difference is the open time, 3, 5 and 9 minutes, respectively. Due to the manual production, mainly the adhesive with the longest open time, 5221, was used for the beams. The adhesive is designed to substitute mechanical fastening techniques in structural and semi-structural bonding, the tensile strength is approximately 10 MPa and the lap shear strength 6-10 MPa, all according to the product data sheet [7]. Further, the data sheet also gives an approximate elongation at break of 150 % and an approximate glass transition temperature of 52°C. In the data sheet it is also noted that the mechanical properties are temperature dependent.

Sikasil SG-500 is a two-component silicone sealant. The adhesive cures by polycondensation and it is UV resistant. One of the main applications of this adhesive is structural glazing [8]. According to the product data sheet the tensile strength is approximately 2.2 MPa and the elongation at break approximately 300 %.

SikaMelt-9676 OT is a one-component polyurethane-based reactive hot-melt. At the application temperature of 110–160°C, the moisture-dependendent curing is initiated. The open time is approximately 6 minutes, the tensile strength is approximately 15 MPa and the lap shear strength 6-10 MPa, all according to the product data sheet [9]. Further, the data sheet also gives an approximate elongation at break of 900 % and a softening temperature of 75°C, but the adhesive has no affirmed UV-resistance.

2.1.2 Substrates

The glass of the I-beam webs was float glass, according to the European standard EN-572, with a thickness of 10 mm and delivered from Pilkington Floatglas AB. For most beams, the glass plates were not further treated after the traditional cutting (snapped along a scratched mark), but for five of the beams, the glass plates were grinded (roughly polished) on the corners of the cross section. In Table 1, these differences are referred to as ‘no finish’ and ‘polished edges’, respectively.

For the wooden flanges, LVL (laminated veneer lumber) with a machined groove was used. Two different groove widths were used. Figure 1 shows the cross-section dimensions and the different flange types.

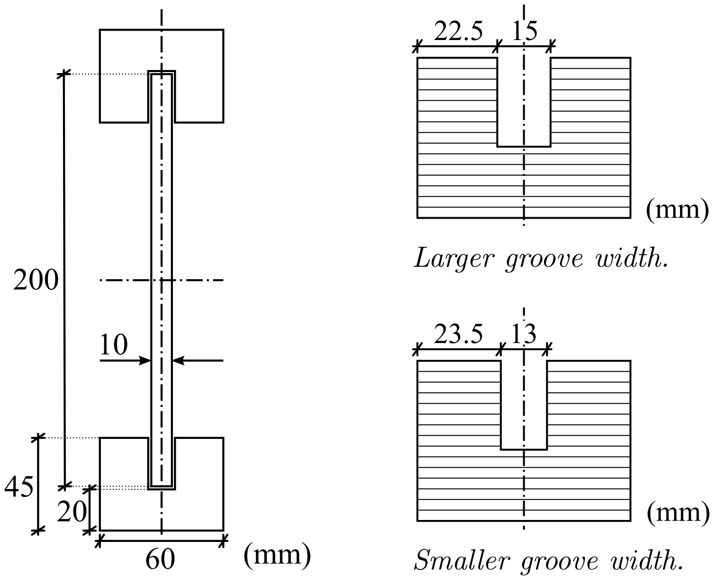

Larger groove width.

Smaller groove width.

Figure 1: Cross section of beam (left) and flange types (right).

2.2 Gluing process

The adhesive was applied manually in the flange groove. For the two-component adhesives equipment designed to mix the components of the adhesive was used, see Figure 2. To ensure that the glass web was centered in the flange groove, spacers,

Table 1: Notation system for the beams.

Adhesive		Flange type		Glass finish	
A	Acrylate	L	Larger groove width	N	No finish
S	Silicone	S	Smaller groove width	P	Polished edges
P	Polyurethane				

Table 2: Notation and numbering of produced specimens.

ALN	$-$ 01, 02, . . . , 07 [a]
ASP	$-$ 01, 02, . . . , 05
SLN	$-$ 01
PLN	$-$ 01

[a] ALN-05 was exposed to hammer-blows during testing

rubber stripes or steel profiles, were used, see Figure 3. After the adhesive was applied and evened out and the spacers in place, the glass web was lowered down into the groove by a vertically adjustable fixing device, see Figure 4. When the adhesive had cured sufficiently, the procedure was repeated for the second flange.

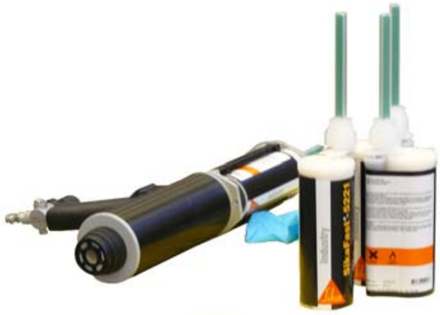

Figure 2: Adhesive application equipment for the two-component adhesives. The greenish top of the adhesive containers is the static mixer where the components are mixed automatically.

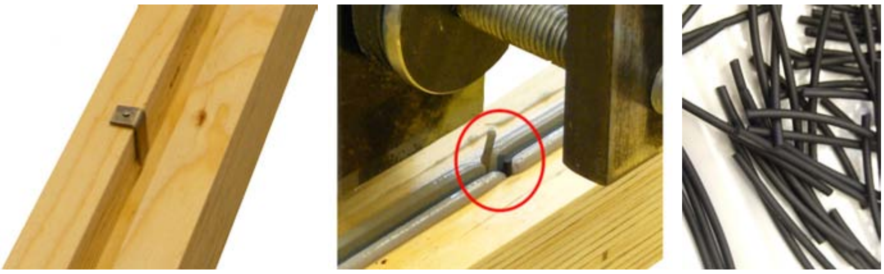

Figure 3: Steel profile spacer (left), a rubber spacer in place (mid) and unattached (right).

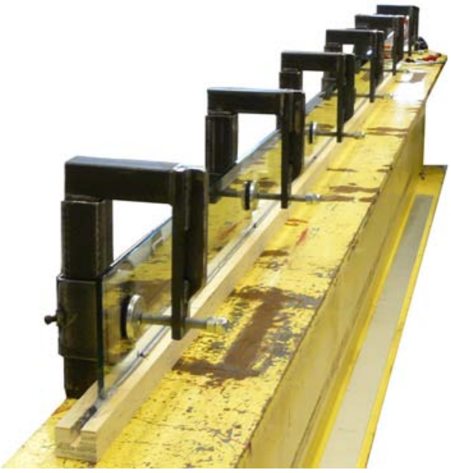

Figure 4: The glass web lowered down into the flange groove.

2.3 Test equipment and procedure

The tests were performed in an electro-mechanical machine, Alwetron TCT 100, with a load-capacity of ±100 kN, Figure 5.

The test procedure was four-point bending with lateral supports along the beam, preventing lateral/torsional buckling and comprised two different tests; a stiffness test with low load levels and the main test where the beams were loaded until failure. Note that the height, $h = 240$ mm, which is referred to, is the nominal height of the beam, not including the increase in height due to the adhesive thickness at the top and bottom of the glass web.

In the stiffness test, the beams were first pre-loaded with 1 kN and then loaded up to 5 kN. The stiffness is calculated from the difference in deflection between these two load levels. Deflection was measured both with a local and a global measure. The global deflection is the mid-point deflection with the whole beam length considered, while the local deflection is measured from the bending of a $5h(= 1200$ mm) long distance in the middle of the beam, see Figure 6 where the local and global deflections are denoted v_{local} and v_{global}, respectively.

In the load-capacity test, the loading is displacement-controlled at a rate of 9 mm per minute. The displacement used to control the loading rate is the one measured by the machine and this is also the only displacement measured in the load-capacity test.

2.4 Bending stiffness calculation

The bending stiffness, EI, where E is the modulus of elasticity and I the moment of inertia, can be calculated from both the stiffness test and the load capacity test. In the latter, the quotient $\Delta P/\Delta v$ is determined by the initial slope of the load-deflection curves. Table 3 shows the resulting expressions for the bending stiffness.

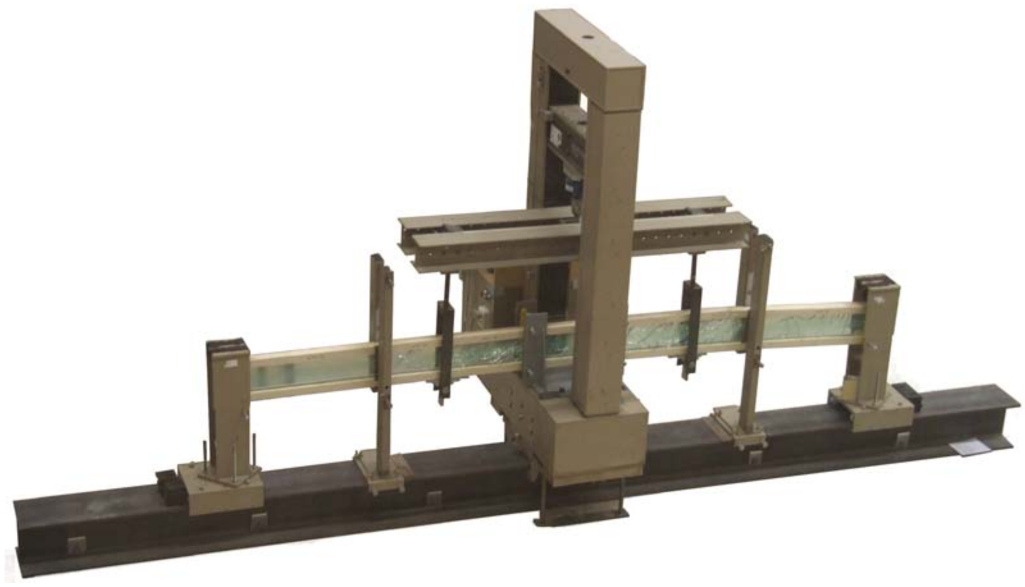

Figure 5: Testing machine.

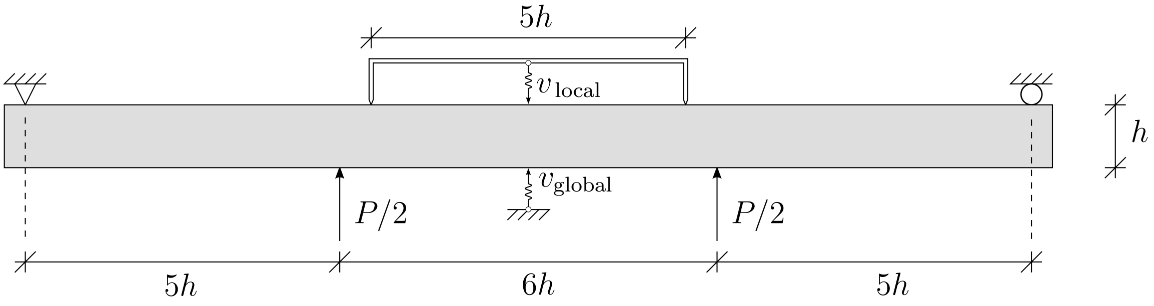

Figure 6: Loading and deflection measures of the beams.

Table 3: Expressions for calculating the bending stiffness of the beams.

Deflection measure	load point	local	global
Bending stiffness	$\dfrac{175h^3\Delta P}{3\,\Delta v}$	$\dfrac{125h^3\Delta P}{16\,\Delta v_{\text{local}}}$	$\dfrac{835h^3\Delta P}{12\,\Delta v_{\text{global}}}$

3 Results

The initial slope of the load–displacement curves in the load capacity test was taken to be the maximal slope of straight lines fitted in the least squares sense to data in 4 kN load intervals. The result was used both to calculate the initial bending stiffness and to shift the curves along the displacement-axis such that the line corresponding to the initial stiffness starts at zero displacement. The load–displacement curves obtained in the load capacity test are shown in Figure 7.

In all specimens, the load at which the first crack appeared was much lower than the maximal load. Several cracks in mostly the glass appeared before the ultimate failure of the beams. Table 4 presents the load where the first crack appeared and the maximal load. The load at first crack is estimated to be at the "first bump" on the load–displacement curve, as this was observed to be typical during the tests.

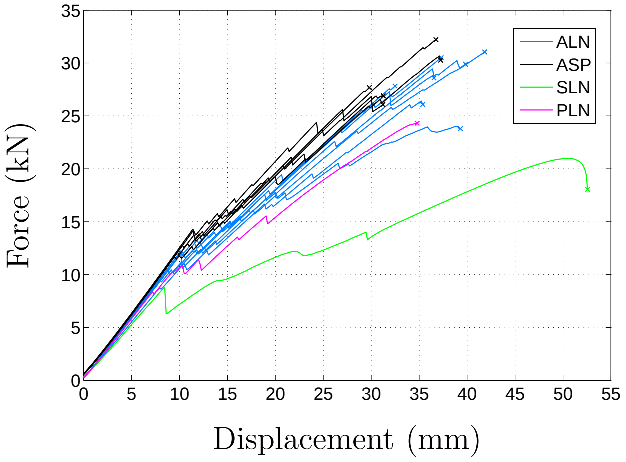

Figure 7: Load–displacement curves for all tested beams.

The stiffnesses presented in Table 5 are the ones obtained from the load capacity test, while Table 6 shows the initial stiffnesses found in the stiffness test. A comparison between the different stiffness measures for each beam can be found in Figure 10 in the Appendix. Figures 11 and 12 show the interval used for the initial stiffness (green dots) and the load at the first crack (dashed red line).

The failure of the beams occurred during a large load interval, cf. Table 4 above, and is initiated at the tension side of the glass where "broom shaped" cracks appear, see Figure 8(a). Later in the failure process, Figure 8(b), the glass breaks more irregularly and at the ultimate load, a failure of the wooden flanges occur as well, Figure 9.

Table 4: Mean values of loads for the tested beams. The standard deviation is denoted by s in the table.

Type	No. of specimens	Load at first crack (kN)	Maximal load (kN)	Increase (%)
ALN	7 pcs.	11.1 ($s = 1.45$)	28.4 ($s = 2.53$)	160
ASP	5 pcs.	13.0 ($s = 1.17$)	28.9 ($s = 2.43$)	120
All acrylate specimens		11.9 ($s = 1.62$)	28.6 ($s = 2.39$)	140
SLN	1 pc.	8.80	21.0	140
PLN	1 pc.	8.37	24.3	190

Table 5: Mean values of stiffnesses for the tested beams. The standard deviation is denoted by s in the table.

Type	No. of specimens	Initial (MNm^2)	Up to maximal load (MNm^2)	Decrease (%)
ALN	7 pcs.	0.954 ($s = 0.029$)	0.617 ($s = 0.061$)	35
ASP	5 pcs.	1.000 ($s = 0.007$)	0.707 ($s = 0.031$)	29
All acrylate specimens		0.973 ($s = 0.032$)	0.655 ($s = 0.068$)	33
SLN	1 pc.	0.850	0.335	61
PLN	1 pc.	0.940	0.564	40

Table 6: The initial stiffnesses (MNm^2) obtained in the stiffness test. The standard deviation is denoted by s in the table.

Type	No. of specimens	Calculated from v_{local}	Calculated from v_{global}
ALN	7 pcs.	1.120 ($s = 0.030$)	1.030 ($s = 0.027$)
ASP	5 pcs.	1.211 ($s = 0.025$)	1.017 ($s = 0.016$)
All acrylate specimens		1.158 ($s = 0.054$)	1.024 ($s = 0.023$)
SLN	1 pc.	1.009	0.918
PLN	1 pc.	1.077	1.021

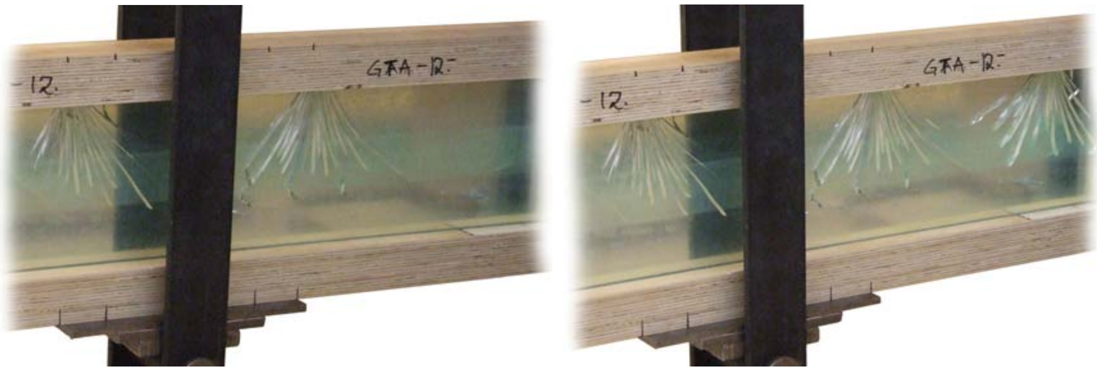

(a) Typical initial crack formations (ASP-05).

(b) Typical crack formation later in test (ALN-03).

Figure 8: Cracks forming during the load capacity test.

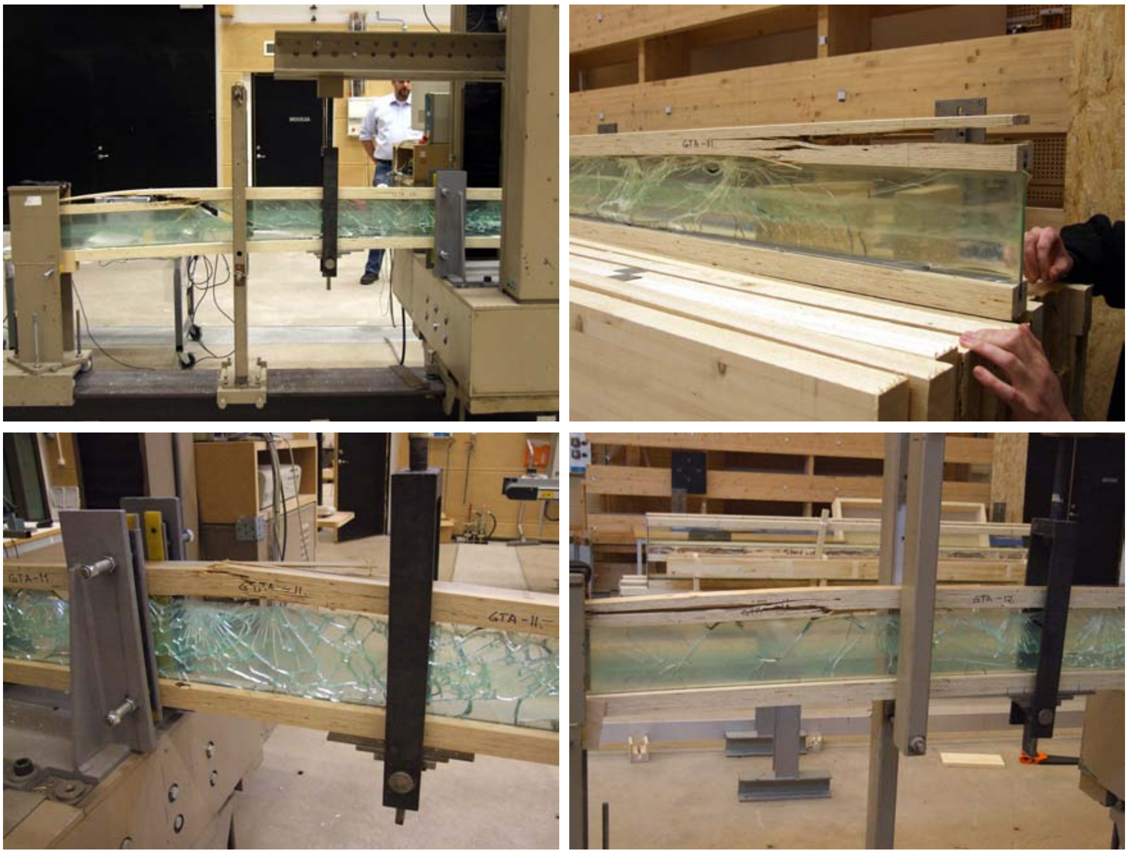

Figure 9: Examples of beams after the final failure.

References

[1] L. Blyberg et al. Timber/Glass Ahesive Bonds. Report 2, Linnæus University, School of engineering, 2010.

[2] J. Hamm. *Tragverhalten von holz und holzwerkstoffen im statischen verbund mit glas*. PhD thesis, EPF in Lausanne, Switzerland, 1999.

[3] K. Kreher. Load introduction with timber, timber as reinforcement for glued composites (shear-walls, I-beams) structural safety a calculation model. In *WCTE*, 2006.

[4] K. Kreher et al. Timber-glass composite girders for a hotel in Switzerland. *Structural engineering international*, 2:149–151, 2004.

[5] P. Louter. Adhesively bonded reinforced glass beams. *HERON*, 52:31–58, 2007.

[6] J. Nielsen and J. Olesen. Mechanically reinforced glass beams. In A. Zingoni, editor, *Recent developments in structural engineering, mechanics and computation*, 2007.

[7] Sika Schweiz AG. Technical Data Sheet, SikaFast 5221, 10 2003.

[8] Sika Schweiz AG. Product Data Sheet, Sikasil® SG-500, 11 2007.

[9] Sika Schweiz AG. Product Data Sheet, SikaMelt®-9676 OT, 11 2008.

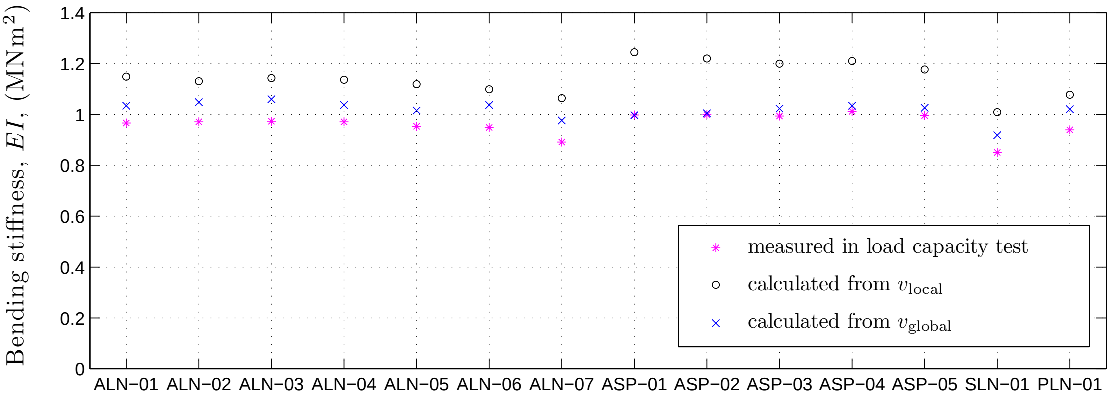

Figure 10: Comparison of the bending stiffness obtained with three different methods.

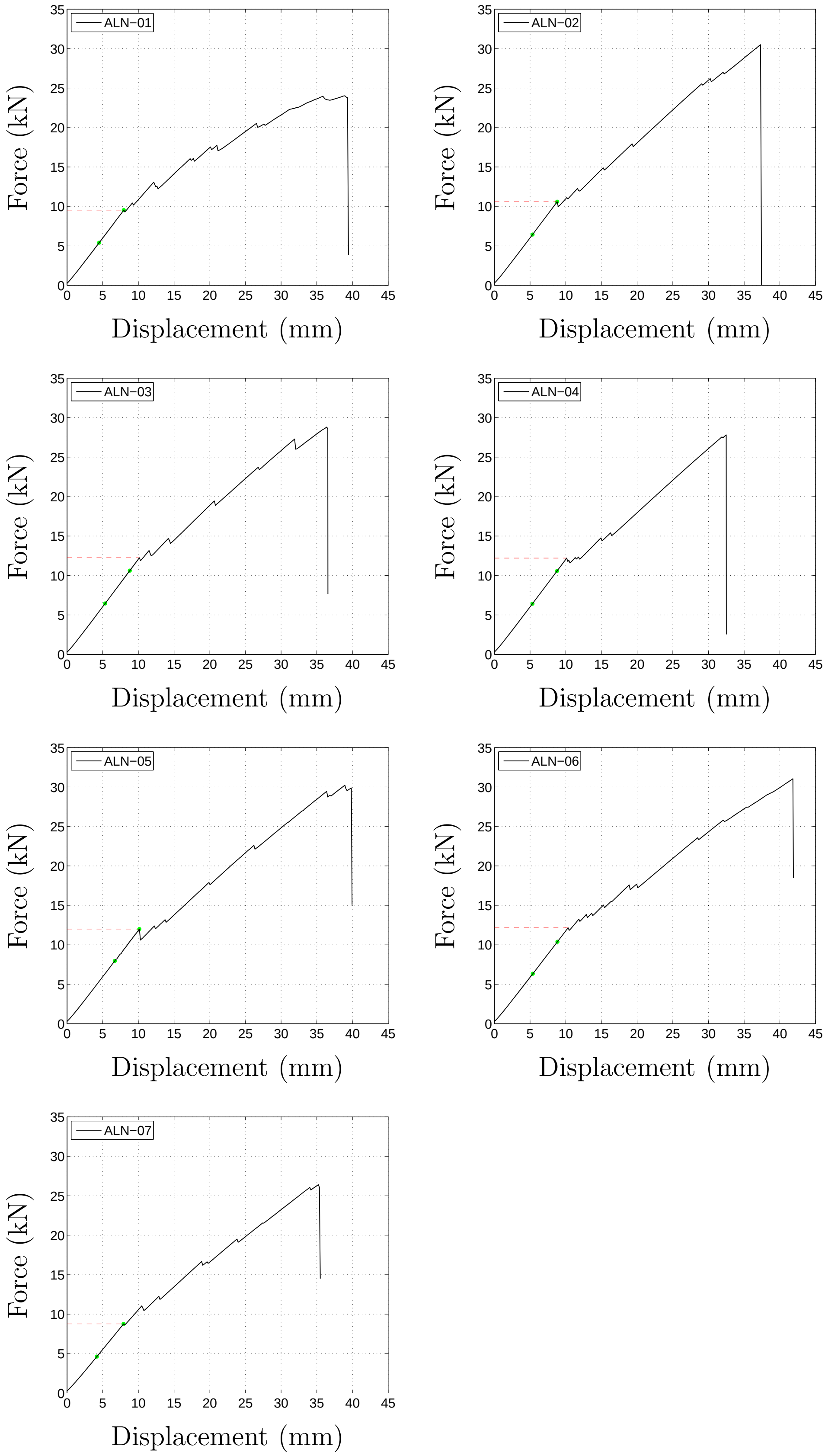

Figure 11: Load–displacement curves for ALN 01-07. The green dots show the interval used to determine the initial stiffness and the red dashed lines the estimate of the load at first crack.

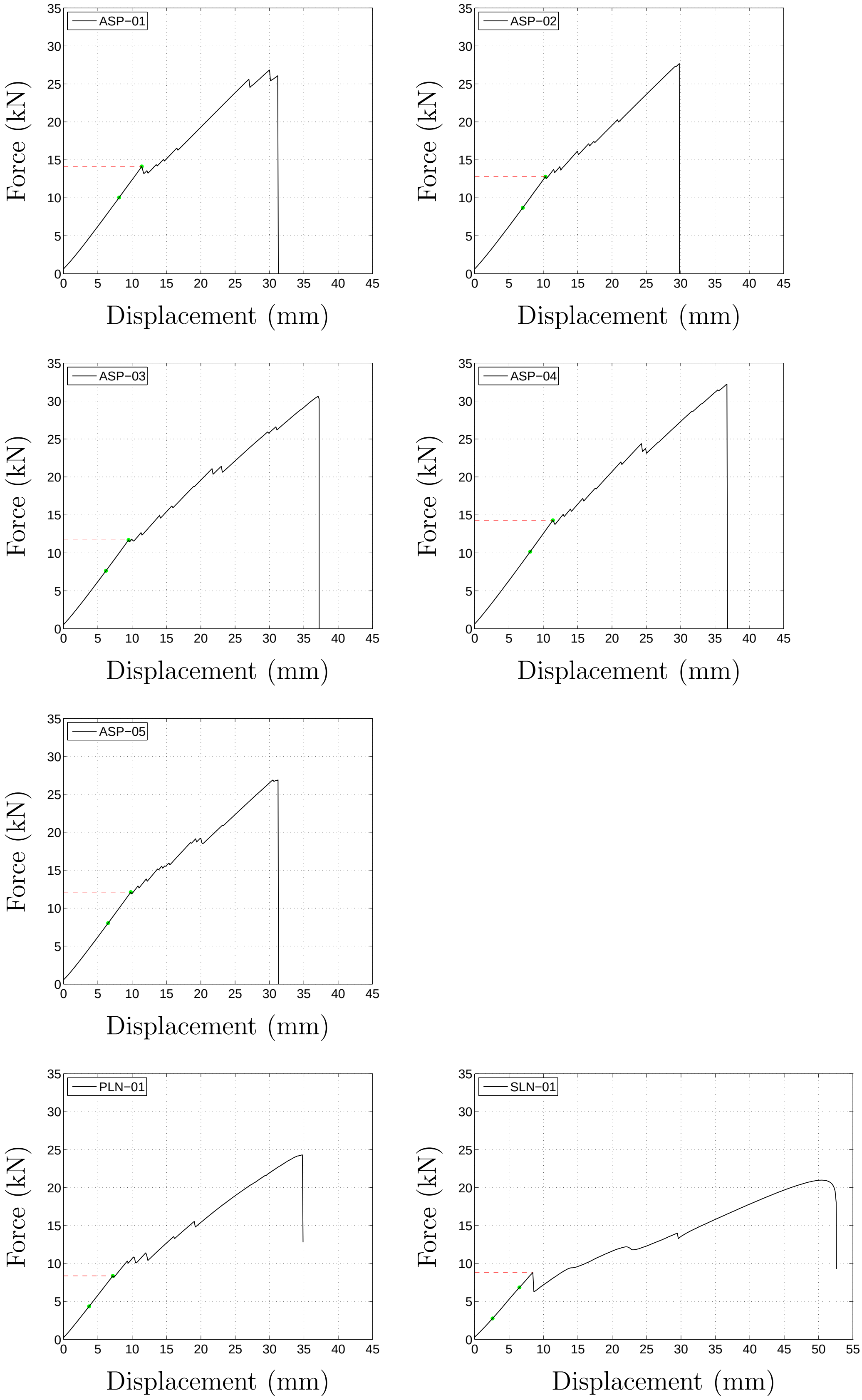

Figure 12: Load–displacement curves for ASP 01-05, PLN-01 and SLN-01. The green dots show the interval used to determine the initial stiffness and the red dashed lines the estimate of the load at first crack.